Chemical Engineering Journal 95 (2003) 123–136

Chemical Engineering Journal

www.elsevier.com/locate/cej

# Improving the flashback resistance of catalytic and non-catalytic metal fiber burners

M. Bizzi, G. Saracco*, V. Specchia

*Department of Materials Science and Chemical Engineering, Politecnico di Torino, Corso Duca degli Abruzzi 24, 10129 Turin (TO), Italy*

Received 9 December 2002; accepted 28 April 2003

**Abstract**

In this paper, the stability and flashback resistance of catalytic and non-catalytic premixed metal fiber burners are investigated by means of a model analysis. The burner model consists of a set of transient conservation equations that account for a detailed kinetic mechanism for the description of methane reactivity in the gas phase. On the side of the catalytic reactivity, the occurrence of a hetero-homogeneous combustion regime sustained by the catalyst activity is assumed. After a preliminary model validation on the grounds of some experiments carried out ad hoc, the mathematical model is used for the analysis of the flashback phenomenon, so as to point out the key parameters that affect burner operation stability. A sensitivity analysis is finally proposed, so as to formulate some general guidelines for the design of improved performance premixed burner. A bi-layer burner structure with smaller pores ahead and larger pores on the downstream side seems to be the way to go in order to enlarge the power modulation range of the burner and improve flashback resistance.


*Keywords:* Porous media; Metal fiber burners; Catalytic combustion; Premixed combustion modeling; Reaction engineering; Natural gas; Flashback

## 1. Introduction

It is well known that premixed radiant burners for natural gas or LPG represent a reliable technology that offers extremely good performance for pollutant emissions and thermal efficiency [1–5]. These devices have been used in a wide range of industrial and domestic applications. They have been employed in the petroleum industry [1], for commercial warm-air furnaces [2], in paper and food industry [3]. Their operation is mainly based on performing the combustion at least in part inside a porous medium. The solid phase receives a large fraction of the chemical energy released by the combustion reactions, which in turn is emitted as radiant energy. The main challenge of these systems is therefore to promote the confinement of combustion inside or close enough the porous medium, so as to maximize the fraction of radiative energy emitted.

The main feature of these burners, compared to traditional ones, is the considerable reduction of the gas-phase temperature that can be achieved operating at a given excess of air and specific power input. This would entail in turn a reduction of thermal $NO_x$ therefore produced.

On the other hand, this cooling may result in a drawback for the CO emission, which might become high especially at the borders of the burners where the sealing systems may exert a further localized cooling. In this context, the catalytic activation of the burner represents the most logical remedy [5]. The catalyst improves the flame stabilization inside the porous medium, allowing an improvement in radiant efficiency. The presence of the catalyst should also allow to expand the range of excess air ($E_a$) in which stable combustion can be achieved and, in particular, it permits richer (but still fuel-lean) combustion mixtures, giving two major consequences:

- The production of nitrogen oxides could be further reduced, since it depends on the square root of oxygen concentration [6]. However, this effect could be partially vanished by the increase in gas-phase temperature occurring at lower excess of air. Practically, nitrogen oxide emissions would be improved by a reduction in $E_a$ in a region close to stoichiometric conditions, whereas at higher $E_a$ the opposite effect would be obtained.
- The thermal efficiency is enhanced, thanks to lower nitrogen mass flow rate.

Finally, the catalyst improves the range-ability of the burner, which is a very important requirement in household applications in the perspective of an energy-saving

* Corresponding author. Tel.: +39-11-5644654; fax: +39-11-5644699.
*E-mail address:* saracco@polito.it (G. Saracco).

1385-8947/$ – see front matter © 2003 Elsevier B.V. All rights reserved.
doi:10.1016/S1385-8947(03)00130-X

**Nomenclature**

| | |
|---|---|
| $a$ | specific area ($m^{-1}$) |
| $\hat{c}_p$ | specific heat ($J\,g^{-1}$) |
| $d$ | diameter (m) |
| $e$ | solid-phase emissivity (–) |
| $E_a$ | excess of air (%) |
| $h$ | volumetric heat transfer coefficient ($J\,K^{-1}\,m^{-3}\,s^{-1}$) |
| $h'$ | area-based heat transfer coefficient ($J\,K^{-1}\,m^{-2}\,s^{-1}$) |
| $\hat{H}$ | enthalpy of a chemical species ($J\,g^{-1}$) |
| $J_E$ | energy flux ($J\,s^{-1}$) |
| $k$ | thermal conductivity ($J\,s^{-1}\,m^{-1}\,K^{-1}$) |
| $K$ | total number of chemical species involved in the reaction environment |
| $L$ | solid-phase domain length (m) |
| $\dot{m}$ | gas-phase mass flow rate ($kg\,s^{-1}$) |
| $m^*$ | effective thermal conductivity modulation factor (–) |
| $M$ | molar weight ($kg\,mol^{-1}$) |
| $\bar{M}$ | mean molar weight ($kg\,mol^{-1}$) |
| $Nu$ | Nusselt number (–) |
| $p$ | pressure (Pa) |
| $Q$ | specific power input |
| $R$ | universal gas constant ($J\,K^{-1}\,mol^{-1}$) |
| $\bar{R}$ | chemical production rate of a species ($mol\,m^{-3}\,s^{-1}$) |
| $Re$ | Reynolds number (–) |
| $S$ | reactor cross section ($m^2$) |
| $t$ | time variable (s) |
| $T$ | temperature (K) |
| $u$ | gas-phase velocity ($m\,s^{-1}$) |
| $V_k$ | diffusion velocity ($m\,s^{-1}$) |
| $[X]$ | molar concentration of a species ($mol\,m^{-3}$) |
| $Y_k$ | mass fraction of species $k$ (–) |
| $z$ | space variable (m) |

*Greek letters*

| | |
|---|---|
| $\Gamma$ | surface adsorption sites concentration ($mol\,m^2$) |
| $\varepsilon$ | porosity (–) |
| $\kappa$ | kinetic coefficient ($m\,s^{-1}$) |
| $\mu$ | gas viscosity ($kg\,m^{-1}\,s^{-1}$) |
| $\rho$ | gas-phase density ($kg\,m^{-3}$) |
| $\sigma$ | Stefan–Boltzman constant ($J\,s^{-1}\,m^{-2}\,K^{-4}$) |

*Subscripts*

| | |
|---|---|
| ads | adsorption |
| eff | effective |
| f | fiber |
| feed | feedstock gas |
| g | gas phase |
| in | solid-phase inlet (upstream surface) |
| $k$ | generic species |
| out | solid-phase outlet (downstream surface) |
| room | ambient conditions |
| s | solid phase |
| surf | surface |
| tr | transport |

*Superscript*

| | |
|---|---|
| $*$ | modulated value |

conduction. Particularly, power modulation ($Q$) from 25 kW needed for hot, sanitary water production (showers, cooking, washing, etc.) down to a few kW for household heating is currently pursued in modern "combi" boilers.

Unfortunately, especially at low $E_a$ and $Q$ values, radiant burners often suffer from stability problems related to flashback and the catalytic ones are even more critical from this viewpoint. After a period of a stable operation, the porous medium reaches so high temperatures that the feedstock is ignited ahead of the porous medium itself, thus giving flashback.

In the present paper, some topics are discussed:

- model set up and validation for both catalytic and non-catalytic premixed burners;
- burner stability and flashback;
- sensitivity of the burner performance to some relevant physical parameters.

A discussion on the principles governing premixed burners was already reported in a previous paper [7], together with a detailed analysis of flashback in non-catalytic metal fiber burners. In this work, the analysis of the fundamental aspects of radiant burners is mainly focused on the differences between catalytic and non-catalytic systems. A quantitative estimate of flashback occurrence is given for both types of burners. Furthermore, a sensitivity analysis offers more insight into the variables one can play upon during the burner design in order to face the reduced stability following the catalytic activation of the porous medium. A series of guidelines are therefore proposed and discussed, and an "optimal" set of design criteria is formulated.

## 2. Experimental

Some experiments have been carried out to support the model analysis here presented. In particular, the surface temperature was measured at different specific power inputs and excess of air values, since it was considered as the most representative variable of the burner operation. Actually, it is clear that radiation is strictly related to the burner surface temperature, thus affecting both performance and flashback occurrence [7].

A detailed description of the experimental apparatus employed in the study has been given elsewhere [8]. Nevertheless, some details are here reported. A boiler of the maximum power of 40 kW is fed with gas streams, air and methane, premixed in a Venturi. The air mass flow rate is determined by a blower and the methane flow rate by a modulating electro-valve. The thermal load required by the user is controlled by modulating the blower speed. A pneumatic-valve, driven by the pressure drop of the gas feedstock throughout the Venturi, changes the natural gas flow rate so as to keep a constant excess air ratio. In other words, as the air flow rate increases, the pressure drop rises, and this signal is used to increase the methane flow rate. Different $E_a$ values can be achieved by playing on the offset and the gain of the valve. In the plenum chamber, the distribution of the gas on the porous medium is accomplished by a system of perforated plates, in order to obtain the gas flow onto the fiber panel with a uniform flow field. The porous medium (a 2 mm thick FeCrAlloy NIT100S fiber mat by ACOTECH, Zwevegem, Belgium) is placed horizontally, at the end of the plenum chamber, and is firing upwards. Beyond this non-catalytic fiber mat, also a catalyzed version of it was tested. A 2 wt.% Pd catalyst supported on $La_2O_3$-stabilized (10 wt.%) $\gamma$-$Al_2O_3$ was prepared and washcoated over the fibers of the burner for such a purpose.

Just above the combustion chamber, the flue gases were cooled through a "finned-tube" type heat exchanger. After some of the flue gases are sampled for composition analysis, they are dispersed through a chimney. The composition of the exhaust gas was monitored by means of a set of continuous Elsag-Bailey analyzers: a $NO_x$ chemiluminescence analyzer, a FT-IR analyzer for CO and $CO_2$, an $O_2$ paramagnetic detector. The surface temperatures of the upstream and downstream burner surfaces were recorded for each test through specific thermocouples placed on the metal fiber mat. Test runs were carried out in the range of specific power inputs from 200 to 800 kW/m$^2$ at different excess of air values (from to 5 to 90%).

For the investigation of the burner stability, $Q$ was modulated stepwise ($\Delta Q \geq 20$ kW/m$^2$) from a stable radiant regime ($Q = 500$ kW/m$^2$) down to occurrence of flashback at selected values of $E_a$. If the burner could work in stable conditions for at least 15 min, flashback occurrence was excluded at the operating conditions ($Q$, $E_a$) under investigation.

## 3. Model

### 3.1. Burner equations

The burner behavior is described by a transient one-dimensional model, consisting of equations for mass continuity, gas-phase species conservation, energy conservation of the gas and the solid phases, and by the ideal gas law. The model accounts for ordinary and thermal diffusion in the gas phase along the longitudinal direction, for inter-phase energy transfer and radiation within the porous medium by an effective thermal conductivity approach [9]. Heat and mass transfer between the porous medium and the gas phase are also considered, using literature transfer coefficient expressions [9]. A summary of the conservation equations is provided in Table 1, with symbol definitions given in nomenclature. Moreover, a complete description of the model and system parameters can be found in [7]. Typical values of the physical parameters employed in the burner simulations are reported in Table 2.

Appropriate boundary conditions are used [3], consisting of fixed values imposed at the domain inlet and of flat profiles at the outlet for the mass fractions and the gas-phase temperature. For the solid-phase temperature, a condition of energy conservation at the upstream boundary is imposed. At the downstream surface, the solid-phase temperature is calculated so as to satisfy an overall energy balance and its value determined the total radiant losses from the burner that

Table 1
Governing equations

Continuity equation

$$\dot{m} = S\rho u \text{ (gas-only region)} \quad (13)$$

$$\dot{m} = S\varepsilon\rho u \text{ (gas-solid region)} \quad (14)$$

Mass balance equation

$$\frac{\partial(S\varepsilon\rho Y)_k}{\partial t} + \dot{m}\frac{\partial Y_k}{\partial z} + \frac{\partial(V_k S\varepsilon\rho Y_k)}{\partial z} - \bar{R}_k M_k S\varepsilon = 0 \ (k = 1, \ldots, K) \quad (15)$$

Gas-phase energy balance equation

$$\frac{\partial(S\varepsilon\hat{c}_{pg}\rho T_g)}{\partial t} + \dot{m}\frac{\partial(\hat{c}_{pg}T)_g}{\partial z} + \sum_{\text{species},k}\frac{\partial(V_k Y_k S\rho\varepsilon\hat{c}_{pg,k}T_g)}{\partial z} + \frac{\partial}{\partial z}\left(-k_g S\varepsilon\frac{\partial T_g}{\partial z}\right) - \sum_{\text{species},k}\bar{R}_k M_k \hat{H}_k S\varepsilon + hS(T_g - T_S) = 0 \quad (16)$$

Solid-phase energy balance equation

$$\frac{\partial(S(1-\varepsilon)\rho_s\hat{c}_{ps}T_s)}{\partial t} + \frac{\partial}{\partial z}\left(-k_{s,\text{eff}}S\frac{\partial T_s}{\partial z}\right) - hS(T_g - T_s) = 0 \quad (17)$$

Equation of state

$$\rho = \frac{p\bar{M}}{RT_g} \quad (18)$$

Table 2
Typical values of the burner physical parameters and operating conditions

| | |
|---|---|
| $Q$ (kW/m$^2$) | 250–600 |
| $E_a$ (%) | 5–35 |
| $p$ (kPa) | 101.3 |
| $S$ (m$^2$) | 0.04 |
| $L$ (m) | $2 \times 10^{-3}$ |
| $d_f$ (m) | $5 \times 10^{-5}$ |
| $e$ | 0.8 |
| $\varepsilon$ | 0.8 |
| $k_{s,eff}$ (W m$^{-1}$ K$^{-1}$) | 0.15–0.30 |
| $h$ (W m$^3$ K) | $1.5 \times 10^6$–$4 \times 10^6$ |

are set equal to the net convective heat transfer from the gas to the porous medium [3].

The model equations are solved by means of a tailor-made simulation software in Fortran language, programmed with the typical architecture of the Chemkin applications. It was also interfaced with the Chemkin [11] and Transport [12] libraries developed at the Sandia National Laboratory.

The chemical reactivity of methane in the gas phase is described by means of a complex combustion mechanism [10], namely the Kazakov–Frenklack mechanism, consisting of 104 reactions among 22 chemical species. This mechanism was deduced by the GRI mechanism [13], and describes the C/H/O chemistry occurring in methane oxidation.

Extensive efforts have been developed to formulate detailed kinetic models of methane reactivity over the surface of different oxidation catalysts, and several mechanisms exist especially for platinum and rhodium based systems [14,15,17]. Unfortunately, the literature lacks of a suitable mechanism of methane reactivity over palladium catalysts, which still remains very uncertain. Besides, this system is known to be very complex mainly due to the presence of active sites of palladium oxide.

In general terms, it could be stated that the catalyst may play in different ways in a catalytic combustor, depending on many aspects such as composition, temperature, pressure, mass flow rate of the feedstock and transport phenomena between the solid and the gas phases. According to the local conditions, the catalytic system may operate in three different situations: (i) the catalyst hosts the combustion on its surface, which is predominantly responsible for the chemical conversion of the feedstock; (ii) the catalyst may assist the combustion, by generating chemical species that are then converted in the gas phase, in a hetero-homogeneous regime; (iii) the catalyst supports the ignition of the combustion in the gas phase, but then the gas-phase reactions can be self-sustained and the role of the catalyst becomes marginal. Generally, the occurrence of one of these regimes is influenced by the local conditions of the feedstock, and determines in turn very different reaction pathways in the overall conversion process. Unfortunately, a very little reliable information can be deduced by experiments, and most of the work that can be carried out in this field is necessarily burdened by this limitation, for any catalyst. This observation is particularly true for the still largely unknown reaction mechanism on palladium catalysts.

It has to be noticed that the formulation of a complete mechanism of methane oxidation on a palladium catalyst is beyond the scope of this work. Therefore, on the basis of the considerations presented so far, a simplified approach is adopted in this paper, based on two experimental observations:

- laser-interferometric measurements on a commercial catalytic burner [16] showed that the presence of the catalyst mainly implies an increment of oxidative radicals in the gas phase (e.g. OH$^\bullet$), if compared to a non-catalytic burner.
- The presence of the catalyst in a metal fiber burner generally determines a reduction in the flashback stability, as showed later in this paper, indicating that the gas-phase reactivity is largely enhanced by the catalyst presence.

The assumption made here is the simplest that allows reproduce these observations. The catalyst is assumed to produce oxidative radicals out of $O_2$ dissociation, promoting a hetero-homogeneous regime. In this way it is possible to explain the larger OH$^\bullet$ concentration in the gas phase, an increased gas-phase reactivity and therefore a reduced flashback resistance.

Naturally, the simple assumption made here is not intended to fully represent the methane reactivity over a palladium surface, which likely would imply a multi-step mechanism among several gas and surface species. Nonetheless, this simple assumption permits to explain the major observed features induced by the catalyst, as mentioned before, in terms of reduced flashback resistance and also in terms of the higher surface temperatures measured in the experiments. Therefore, this assumption has to be intended like a “fitting” condition that allows account for the catalyst activity in a very simple manner, so as to draw some major conclusions consistent with the physical phenomena observed in practice.

To go more in detail in describing our approximation of the catalyst role in the conversion process, the oxygen molecules are assumed to migrate towards the active sites, at a rate depending on both transport and chemical kinetics, and then to be dissociated into O$^\bullet$ radicals at the catalyst surface according to the following reaction:

$$O_2 \rightarrow 2O^\bullet \tag{1}$$

The rate constant of reaction (1) is given as [12,17]

$$\kappa_{ads,O_2} = \frac{0.01}{\Gamma}\sqrt{\frac{RT}{2\pi M_{O_2}}} \tag{2}$$

where the surface site density was assumed to be $2.7 \times 10^{-9}$ mol/cm$^2$ [17]. The rate parameters adopted here have been assumed from a study carried out on rhodium and platinum catalysts in partial oxidation reactions, since data on palladium were not available.

The transport velocity is calculated by the Colburn analogy [18]:

$$\frac{Nu}{Re\,Pr^{1/3}} = \frac{Sh}{Re\,Sc^{1/3}} \tag{3}$$

using the energy transfer coefficients presented in [3]

$$Nu = 0.04Re^{0.53} \quad (Re < 0.4),$$
$$Nu = 0.10Re^{1.64} \quad (Re > 0.4) \tag{4}$$

where

$$Re = \frac{\dot{m}d_f}{S\mu_g} \tag{5}$$

Making the proper substitutions, the Sherwood number can be expressed as

$$Sh = 0.04Re^{0.53}\left(\frac{Sc}{Pr}\right)^{1/3} \quad (Re < 0.4),$$
$$Sh = 0.10Re^{1.64}\left(\frac{Sc}{Pr}\right)^{1/3} \quad (Re > 0.4) \tag{6}$$

From these expressions, the mass transfer coefficient $\kappa_{tr}$ can be determined.

The combination of these equations is based on the consideration that both phenomena are first order in the oxygen concentration. The resulting rate equation for oxygen transport/adsorption/dissociation therefore accounts for both the surface temperature and mass flow rate and is as follows:

$$\bar{R}_{O_2,surf} = \frac{a}{1/\kappa_{ads} + 1/\kappa_{tr}}[X_{O_2}] \tag{7}$$

The surface is then assumed to operate in quasi-steady-state conditions, i.e. no accumulation is possible on the active sites. Therefore the oxygen radicals formed as a result of $O_2$ migration and dissociation are consequently released in the gas phase. Then, the radicals take part in the gas-phase reactivity, initiating the oxidation mechanism. In the following paragraphs, it will be numerically demonstrated that the heterogeneous generation of $O^\bullet$ radicals entails in turn a remarkable increment of $OH^\bullet$ radicals concentration inside the porous medium. Moreover, it will be shown that the catalyst determines an increase in the porous medium surface temperature and a reduction in the flashback resistance, as experimentally observed.

### 3.2. Burner stability

The analysis of the burner stability and flashback was carried out with the following method. The simulation was performed at specific values of the excess of air ($E_a$) and the specific power input ($Q$), until a steady-state solution is found. The inlet gas temperature, initially set to 300 K ($T_{room}$), was stepwise increased and the corresponding new steady-state solutions were determined. The model solutions have been found adopting a continuation procedure, in which each calculated solution has been used as a starting point for the next simulation. By this method, the dependence of the upstream burner surface temperature on the inlet gas temperature was observed, and $T_{s,in}$ versus $T_{g,feed}$ patterns were plotted. The feedstock pre-heating and therefore the inlet gas temperature are then related to the upstream surface temperature. An energy conservation equation can be written by considering that the radiant flux in the backward direction determines the pre-heating of the feedstock:

$$\dot{m}\hat{c}_p(T_{g,feed} - T_{room}) = S\sigma e(T_{s,in}^4 - T_{room}^4) \tag{8}$$

The equilibrium solutions of the system were obtained by coupling this equation with the $T_{s,in}$ versus $T_{g,feed}$ pattern. The inlet gas temperature and the upstream surface temperature are those that simultaneously satisfy the $T_{s,in}$ versus $T_{g,feed}$ pattern and Eq. (8).

## 4. Results and discussion

### 4.1. Model validation

The first step in our analysis was the model validation. Since a crucial point in the behavior of these systems is the heat exchange between the gas and the solid, attention was focused on the metal fiber mat surface temperature. As previously described, experimental measurements were carried out to inspect the variation of the surface temperatures with specific power input and excess of air. Fig. 1 represents the comparison between model calculations and experimental temperatures of the downstream burner surface, with a comparison between the values of a non-catalytic system (black colored [7]) and those of the porous medium catalytically activated with palladium (gray colored). Results concerning the occurrence of flashback are also indicated on the picture: open symbols indicate that flashback takes place within 15 min of operation at the given operating conditions. The results show that the catalyst increases the surface temperatures of the porous medium, thus entailing an improvement in the system behavior thanks to enhanced radiation. On the other hand, the increased temperature level of the porous medium determines a reduction of the burner stability, which is clearly indicated by flashback occurrence at $Q$ values higher than those typical of a non-catalytic burner.

The typical shape of the temperature profiles can be explained with the help of Figs. 2 and 3, revealing some major features induced by the catalyst. The calculated profiles along the non-catalytic burner are shown in Fig. 2. The system exhibits two distinct regions: at the gas inlet the porous medium pre-heats the gas, which is ignited as the temperature reaches a sufficiently high value. When the release of the combustion energy occurs, the gas temperature overcomes that of the solid and the inter-phase heat flux is inverted, with the solid receiving energy from the gas phase. As shown in Fig. 1, the downstream surface temperature rises with $Q$ up to a maximum as a result of a higher net energy

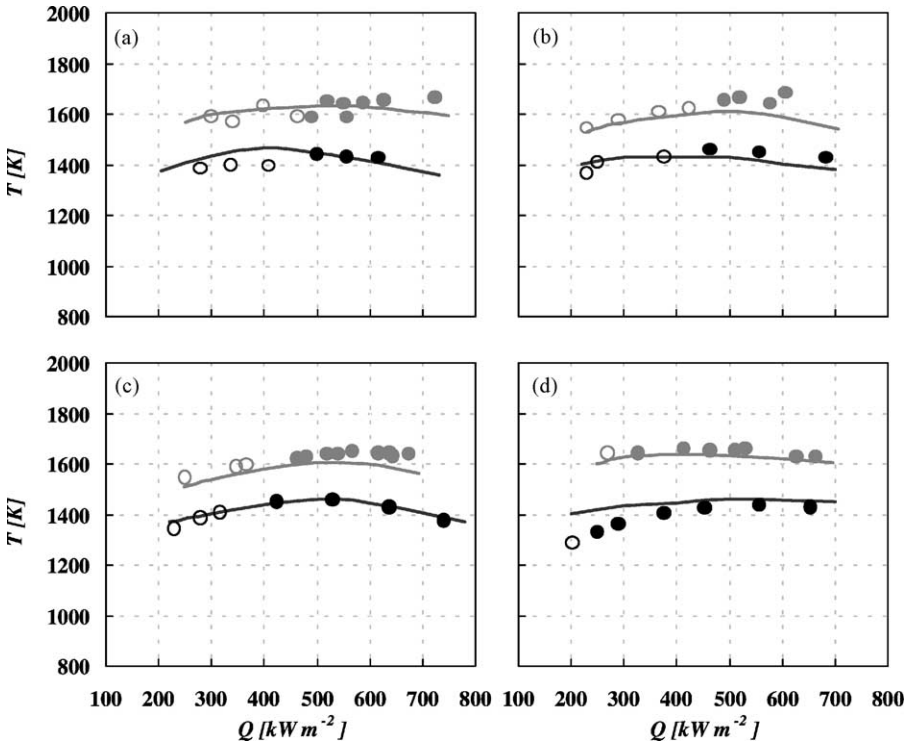


Fig. 1. Downstream burner surface temperature. Comparison between experimental data and model calculations. Excess of air values: (a) $E_a = 5\%$; (b) 10%; (c) 15%; (d) 30%. Empty symbols: flashback experimentally observed within 15 min. Closed symbols: no flashback observed. Gray symbols: catalytic burner; black symbols: non-catalytic burner [7].

input in the porous medium. However, it can be demonstrated that the concentration profiles move downstream as $Q$ is increased [7] and, due to the reduced contact time, the gas pre-heating is penalized. As a consequence, the region of gas pre-heating is expanded and the reaction ignition is delayed. The reaction zone inside the porous medium therefore is reduced and moves towards the exit surface. Part of the energy that could be exchanged with the porous medium actually remains confined in the gas phase, due to the reduction in the contact time between the two counter parts. When the reaction zone reaches the exit surface, the oxidation reactions are far from completion inside the porous medium thus determining a solid-phase temperature decrease. With a further increase in mass flow rate, a partial flame lift off occurs and a "blue flame" regime is settled.

The thermal profiles of the catalytic burner shown in Fig. 3a reveal a major difference induced by the catalyst. The initiation of the radical oxidation process takes place on the catalyst surface at relatively low temperatures, so that the gas feedstock does not need a remarkable pre-heating to reach ignition. As a consequence, the solid-phase temperature remains, at least for the conditions to which the calculations are referred to, below the gas-phase one. The oxidation reactions in the gas-phase start at lower temperatures thanks to the beneficial effect of oxygen radicals generation by the catalyst (hetero-homogeneous reaction pathways). As for the non-catalytic burner, an increase in $Q$ determines an increment of the energy input in the system, which therefore results in increased surface temperatures (Fig. 1). Once again, after a temperature maximum has been reached, the rise in $Q$ finally results in a decrease of the system temperatures, due to the reduction in the contact time between the gas and the solid.

Fig. 2b and c shows the typical concentration profiles along the porous medium length. The reactions start with the production of oxidative radicals, such as $O^\bullet$ and $OH^\bullet$ which in turn react with methane thus promoting the formation of intermediate combustion products (CO, $H_2$). The intermediate products are then converted into $CO_2$ and $H_2O$. In the catalytic burner (Fig. 3b and c), the peak of $O^\bullet$ and $OH^\bullet$ radicals is shifted inside the porous medium as a result of the catalyst activity. This effect, that was experimentally observed on a commercial burner [16], allows to explain the general temperature increment taking place in the system, since the flame front is stabilized inside the porous medium to a significant extent.

The improvement in performance produced by the catalyst is remarkable, in terms of thermal efficiency and pollutant emissions. However, as above underlined, the stability of catalytic burners may be critical in some cases. To further enlighten this point, the analysis of the flashback was carried out.

The first step of the flashback analysis is to find the dependence of the model solution on $T_{g,feed}$, at fixed values of $E_a$ and $Q$. The dependence on $T_{g,feed}$ of the molar fraction of methane $X_{CH_4,in}$ at the upstream surface of the non-catalytic

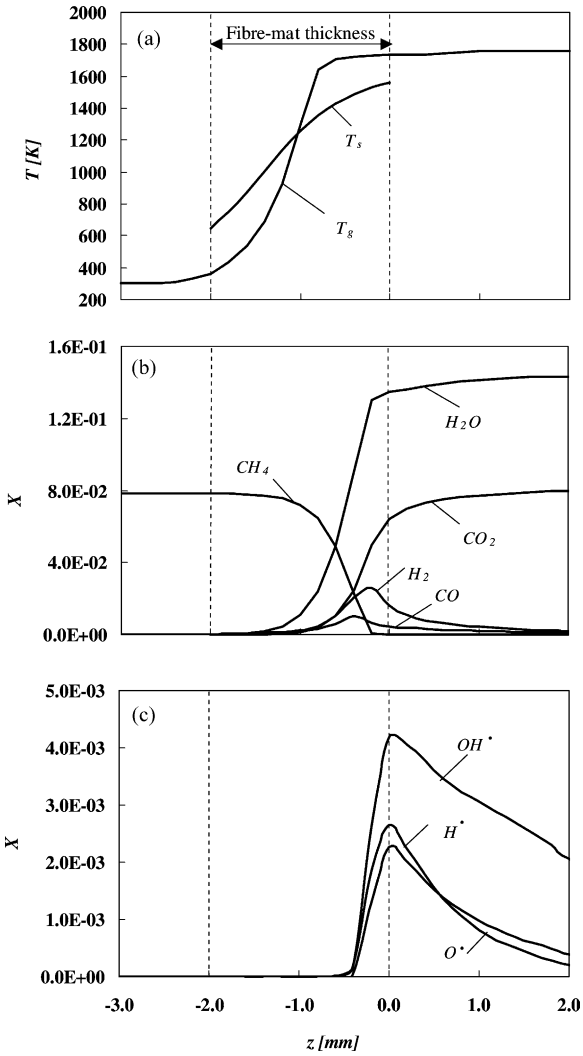


Fig. 2. Thermal and composition profiles calculated for the non-catalytic burner model ($Q = 500\,\mathrm{kW/m^2}$, $E_a = 15\%$): (a) thermal profiles; (b) molar fraction profiles of the principal reactants and products; (c) molar fraction profiles of some radical species.

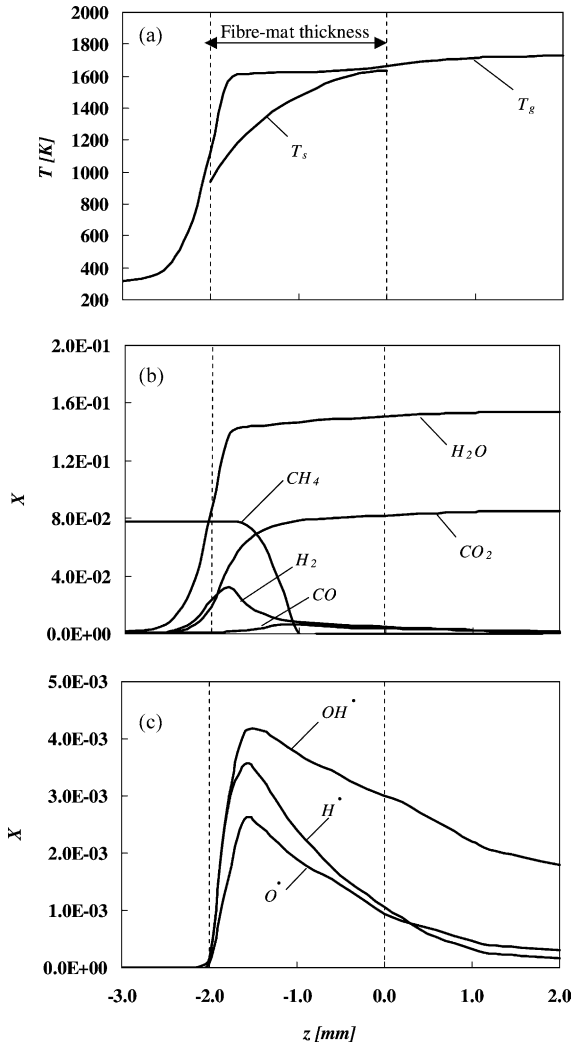


Fig. 3. Thermal and composition profiles calculated for the catalytic burner model ($Q = 500\,\mathrm{kW/m^2}$, $E_a = 15\%$): (a) thermal profiles; (b) molar fraction profiles of the principal reactants and products; (c) molar fraction profiles of some radical species.

porous medium was plotted in Fig. 4. As $T_{g,feed}$ is increased, the reactivity of the gas phase is enhanced and this determines a shift of the concentration profile of methane in the upstream direction. Thus, the methane molar fraction at the upstream burner surface $X_{CH_4,in}$ decreases. Once $T_{g,feed}$ reaches a sufficiently high value, $X_{CH_4,in}$ steeply drops giving indication that the flame front stabilizes ahead of the porous medium. The behavior of the $X_{CH_4,in}$ versus $T_{g,feed}$ curve strongly depends on the specific power input, since at higher $Q$ values the flame front naturally shifts downstream at otherwise constant conditions, hence improving the resistance of the system towards flashback. Similar considerations hold if one considers the dependence of the system behavior on the feedstock composition (Fig. 4a and b). Actually, it can be noticed that a lean mixture determines an increase in the system stability, i.e. higher $T_{g,feed}$ are required for flashback occurrence. To summarize, the system exhibits a more critical behavior in the region of low specific power inputs and low excess of air, i.e. the system becomes more critical in a fully developed radiant heat mode.

The upstream surface temperature of the porous medium was plotted versus $T_{g,feed}$ in Fig. 5, at different values of $Q$. Observing each of the sigmoid shaped curves, it can be noticed that the surface temperature rises with $T_{g,feed}$ and when flashback occurs a steep increase takes place. In the same diagram, the parabolic shaped curves representing Eq. (8) were reported. The intersections of these curves give the possible asymptotic solutions of the physical system, and typically up to three points can be singled out: a stable low-temperature solution, a stable high-temperature solution corresponding to flashback occurrence and an unstable solution. At high values of the specific power input, the sigmoid shaped curves slide on the right side, indicating an improved resistance to flashback. Moreover, at higher $Q$

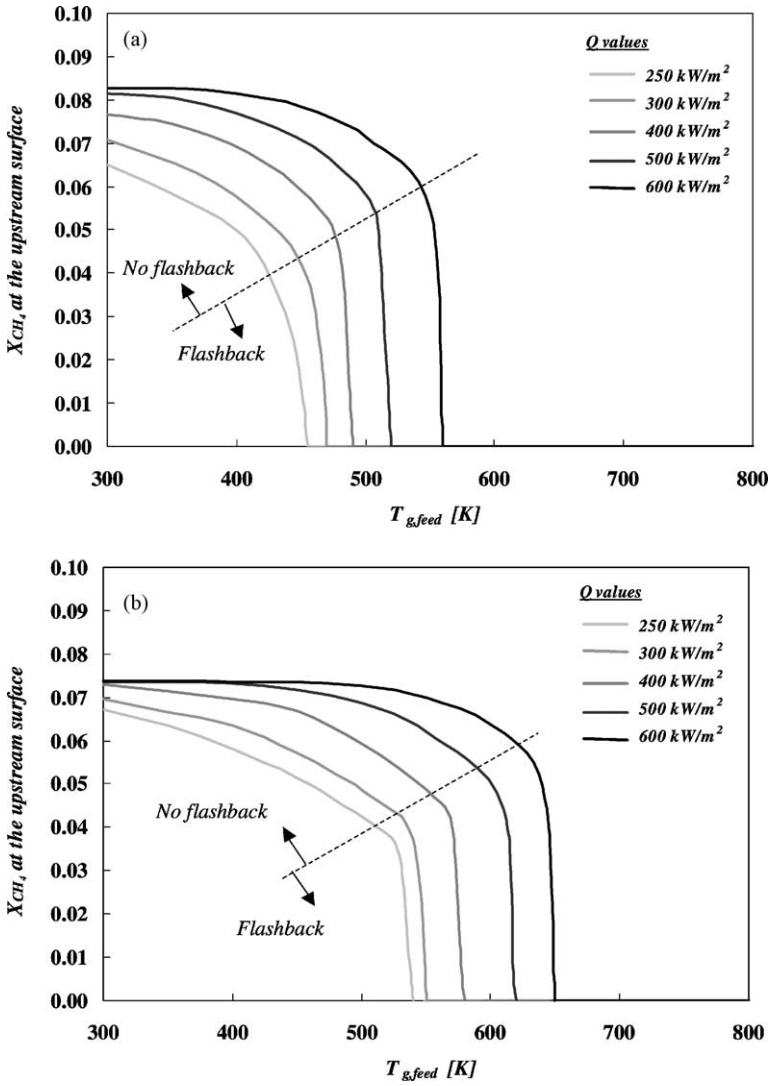


Fig. 4. Calculated methane molar fraction at the upstream burner surface versus inlet gas temperature at various $Q$ values for the non-catalytic burner: (a) $E_a = 15\%$; (b) 30%.

values, the same radiation flux determines a lower feedstock pre-heating, as stated by Eq. (8). As a result, the parabolic shaped curves shift to the right. By observing the intersections reported in Fig. 5a, it can be noticed that the model predicts at high $Q$ values a single "safe" physical solution and at low values a single flashback solution. The transition between these regimes takes place through a multiple solutions region. Physically, this means that the system normally operates in a safe regime, but if an inlet temperature disturbance occurs the burner may evolve towards flashback.

By a systematic analysis of the model results, the limits of safe operation, flashback and steady-state multiplicity (transition) were determined. The results have been summarized in a single "flashback chart", using $Q$ and $E_a$ as key-variables (Fig. 6). The picture reports also a comparison between experimental data and calculations; it can be noticed that the trends observed in practice are clearly reproduced by the model for both the catalytic and the non-catalytic burner. As previously mentioned, the catalyst helps stabilize the flame inside the porous medium. This determines a broad increase of the system temperatures, which is responsible for a reduction of the resistance to flashback. Therefore it can be observed that the curve limiting the region of safe operation moves in the right direction as a result of the catalyst activity.

The improvement of flashback resistance is a goal of crucial importance in burner technology, for non-catalytic and especially for catalytic systems for both industrial and domestic appliances. For example, the current trend in burner technology for domestic applications is to obtain hot water for sanitary purposes and household heating by the same device, which therefore needs to be operated on an "always-on" basis. The burner operates in radiant heat mode for most of the time, providing the energy necessary for the household heating, whereas blue flame mode operation is intended only to satisfy the peaks in the energy demand corresponding to the need for hot sanitary water. In this context, it is crucial

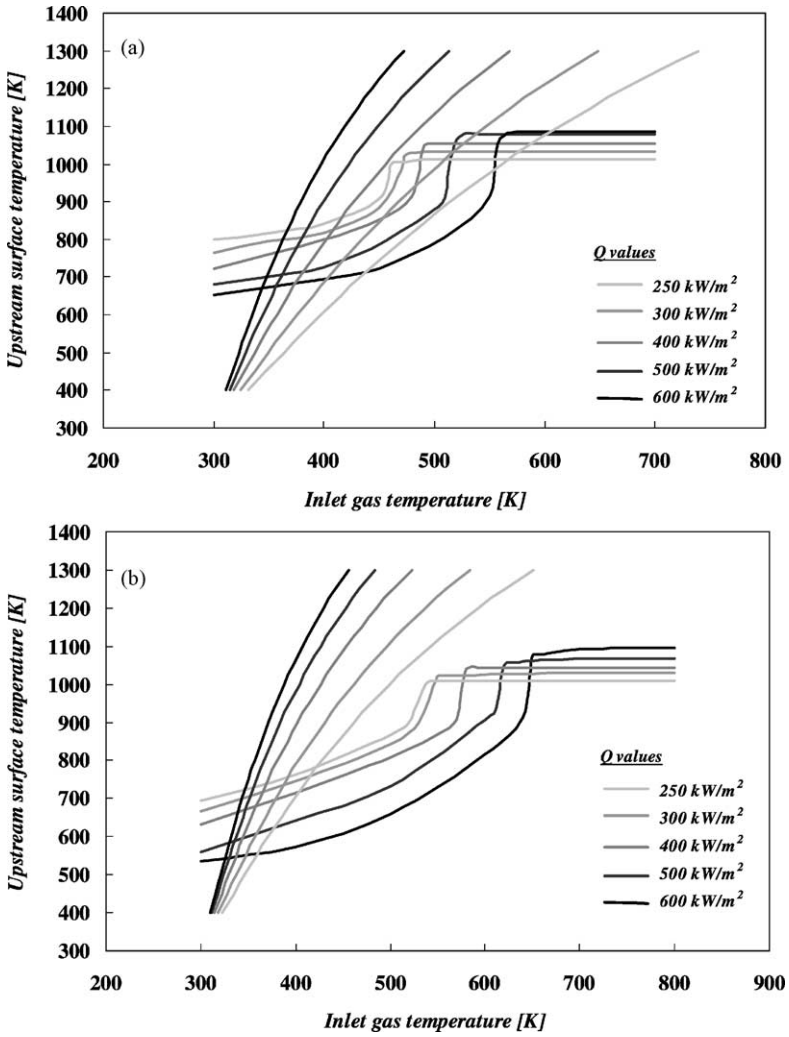


Fig. 5. Calculated upstream surface temperature versus inlet gas temperature at various $Q$ values for the non-catalytic burner: (a) $E_a = 15\%$; (b) 30%.

to understand the mechanisms that enhance stable operation. Moreover, as it has been already noticed, the catalytic activation of the metal fiber determines a remarkable reduction of pollutant emissions, with a significant enhancement in thermal efficiency [19]. The principal drawback of the catalytic activation resides, however, in the related increase in system temperatures, which exert a negative effect on the burner stability. The improvement in flashback resistance therefore is critical also from this standpoint. In the next paragraph, a sensitivity analysis is presented in order to single out some major drivers to improve the burner resistance to flashback.

### 4.2. Sensitivity analysis

To understand the major drivers to enhance the burner stability, a sensitivity analysis has been carried out on four design parameters: metal fiber diameter, porous medium porosity, solid-phase emissivity and thermal conductivity. According to the considerations proposed so far, the resistance to flashback gets worse as the upstream burner temperature increases, all other parameters being constant. For this reason, the analysis considered the dependence of this variable on the variation of the above selected design parameters. The analysis was carried out by means of a continuation procedure, i.e. the model solution for each parameter value was determined from the last calculated one.

Fig. 7 represents the calculated dependence of the upstream and downstream surface temperatures of the non-catalytic porous medium on the fiber dimension $d_f$. It can be observed that the upstream surface temperature remains nearly unaltered when $d_f$ is varied, whereas the downstream surface temperature increases as $d_f$ is decreased, especially at high values of mass flow rate. The fiber diameter influences the heat transfer coefficient [3,7,9]. Solving the heat transfer coefficient equations with respect to the heat transfer coefficient, one obtains

$$h = \frac{1}{d_f^{2-0.53}} \left[ 4k_g(1-\varepsilon)0.04 \left( \frac{\dot{m}}{\mu_g} \right)^{0.53} \right] \quad (Re < 0.4) \qquad (9)$$

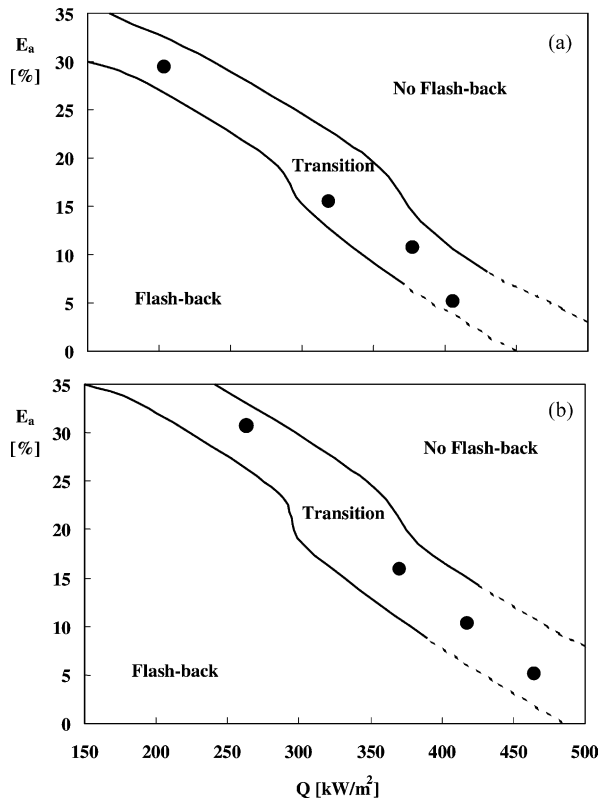


Fig. 6. Flashback charts for the non-catalytic (a) and the catalytic (b) burners. The symbols indicate the starting point of flashback occurrence according to the data plotted in Fig. 1.

$$h = \frac{1}{d_f^{2-1.64}} \left[ 4k_g(1-\varepsilon)0.10 \left( \frac{\dot{m}}{\mu_g} \right)^{1.64} \right] \quad (Re > 0.4) \tag{10}$$

The maximization of the heat transfer coefficient, obtained by a reduction of $d_f$, determines an increase in the fraction of energy transferred to the solid and therefore in the downstream surface temperature. Despite this interesting conclusion for the burner design, the upstream surface temperature remains nearly unaltered and no significant advantage on flashback resistance can be obtained by this way. Besides, it is not possible to reduce the fiber dimensions without paying in terms of long term thermal resistance of the porous medium.

The influence of porosity is represented in Fig. 8, indicating that an increase in this parameter determines a broad increment of the surface temperatures. This conclusion can be explained by considering that higher void fractions facilitate the stabilization of the flame front inside the burner, as a consequence of a decreased linear velocity of the gas phase at constant mass flow rate. Though advantageous for the burner performance, this effect results in an increase of both the upstream and downstream surface temperatures and therefore the resistance to flashback would be diminished.

Fig. 9 summarizes the results of the sensitivity analysis performed on the burner emissivity. This parameter influences the radiation flux emitted at each burner surface, which could be calculated according to the following relation:

$$J_E = \sigma e (T_s^4 - T_{room}^4) S \tag{11}$$

It has to be pointed out that the real value of the energy flux by radiation could be higher than that calculated by Eq. (11), since the contribution to radiation of internal fibers having a non-zero view factor with the thermal load could be important. This issue addresses a more detailed experimental analysis. Higher emissivity values determine improved radiation from the surface, whose temperature therefore decreases as represented in Fig. 9. Therefore, an optimal burner design should maximize emissivity at the burner downstream surface to improve the burner performance. On the other hand, emissivity should be minimized at the upstream surface temperature to prevent flashback. The authors are aware that some commercial premixed burners based on ceramic mullite foams (Ecoceramics, The Netherlands) do carry, deposited on the downstream surface, an emissivity-promoting material based on transition metal oxides. This material is

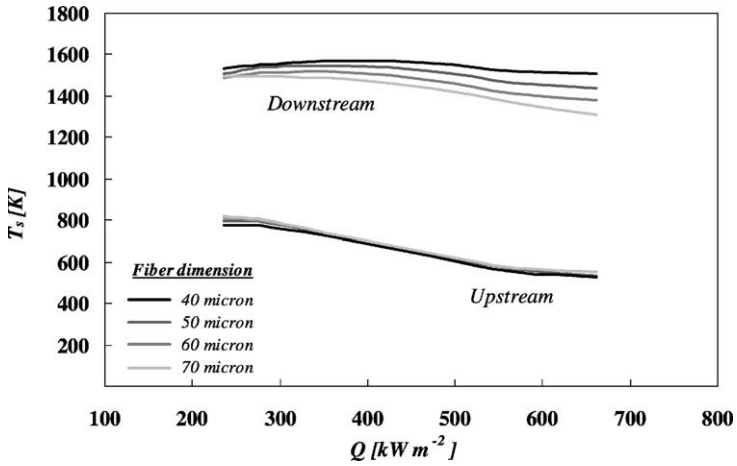


Fig. 7. Influence of the fiber diameter on the non-catalytic burner surface temperature ($E_a = 20\%$).

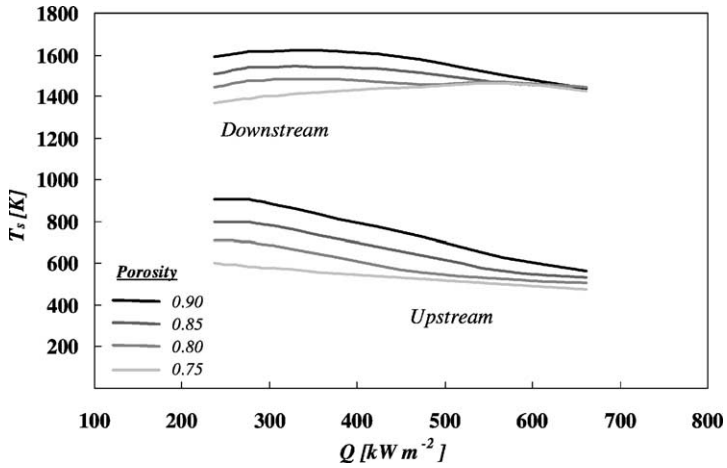


Fig. 8. Influence of porosity on the non-catalytic burner surface temperature ($E_a = 20\%$).

deposited to slightly reduce the $T_s$ value and prolong the lifetime of the burner structural material.

Finally, the influence of effective thermal conductivity was assessed. In this analysis, the $k_{s,eff}$, determined according to the prescriptions listed in [9], was multiplied by a modulation factor $m^*$:

$$k^*_{s,eff} = k_{s,eff} m^* \quad (12)$$

and the model results thus obtained were reported in Fig. 10. It can be noticed that reducing effective thermal conductivity determines a reduction of the porous medium temperatures, at sufficiently high $Q$ values. As the flame front moves upstream (low $Q$ values), the heat released by combustion cannot be dispersed backwards to a large extent along the axial direction in case of a low thermal conductivity and the upstream surface temperature rises.

To summarize, low effective thermal conductivity could decrease the upstream direction energy flux, and therefore the surface temperature, thus improving flashback resistance. However, extremely low values of $k_{s,eff}$ could preclude the gas pre-heating and thus the stabilization of the flame front inside the porous medium, thus preventing the efficient operation of the burner. Hence a trade-off condition between improved resistance to flashback and flame stabilization needs to be found to achieve an optimal configuration.

The results proposed so far give indications to formulate an optimal criterion for the burner design. An optimal porous mat structure should be characterized by a small fiber diameter to improve the heat transfer within the porous medium. A high value of emissivity of the downstream surface favors the radiant efficiency, whereas the emissivity of the upstream surface temperature should be minimized to improve flashback stability. Small values of porosity determine improved resistance to flashback but high pressure drop. A trade-off should be achieved in this case, too. Similar considerations hold as far as the thermal conductivity is concerned, since high values of this parameter determine considerable stabilization of the flame front inside the porous medium and reduce resistance to flashback. It has to be finally noted that the variables analyzed so far are often inter-related so that

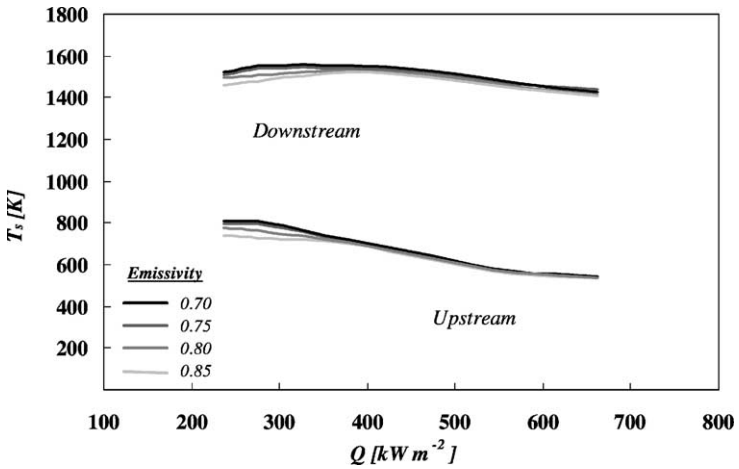


Fig. 9. Influence of emissivity on the non-catalytic burner surface temperature ($E_a = 20\%$).

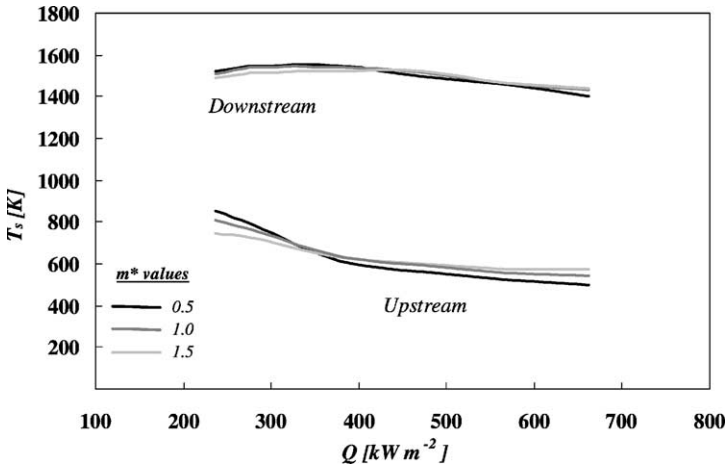


Fig. 10. Influence of effective thermal conductivity on the non-catalytic burner surface temperature ($E_a = 20\%$).

it becomes impossible to control each parameter separately. However, the present discussion is intended to enlighten the effects of the single design parameters on the system performance so as to provide guidelines for an optimal porous mat structure design, which should be carried out respecting the available degrees of freedom and the practical relationship between variables.

### 4.3. Double-layer structure

On top of a correct selection of these design variables, another improvement in flashback resistance could arise from the use of a "radiation shield", to prevent the feedstock pre-heating by radiation. Therefore, a double-layer porous medium has been investigated. The upstream layer is the radiation shield, and since it should maximize the flashback resistance, it should be characterized by low porosity, low thermal conductivity and low emissivity. The downstream layer on the other hand should be designed to maximize the flame front stabilization inside the porous medium and the downstream surface temperature. Accordingly, a high porosity, high thermal conductivity and high emissivity should be employed. The layers are closely interconnected, so that a discontinuity is generated inside the unique non-uniform solid phase. A summary of the parameters of the double-layer structure is reported in Table 3.

The results of a simulation made on the double-layer configuration are reported in Figs. 11 and 12. It can be observed in Fig. 11 that the flame front is somewhat blocked at the interface between the distinct regions, due to the presence of a poorly conductive layer. Therefore, the flashback resistance is greatly improved at constant downstream temperature. Fig. 12 shows the decrease in the system temperatures entailed by the composite porous medium. The upstream surface temperature decreases if compared to the single-layer structure, except at very low $Q$ values; in these conditions, the flame front stabilizes in the upstream layer and its low

Table 3
Double-layer structure parameters

| Design parameter | Upstream layer (radiation shield) | Downstream layer |
|---|---|---|
| Thickness (mm) | 1 | 1 |
| Emissivity | 0.7 | 0.8 |
| Porosity | 0.7 | 0.8 |
| Thermal conductivity | 25% of downstream layer | Calculated according to [9] |

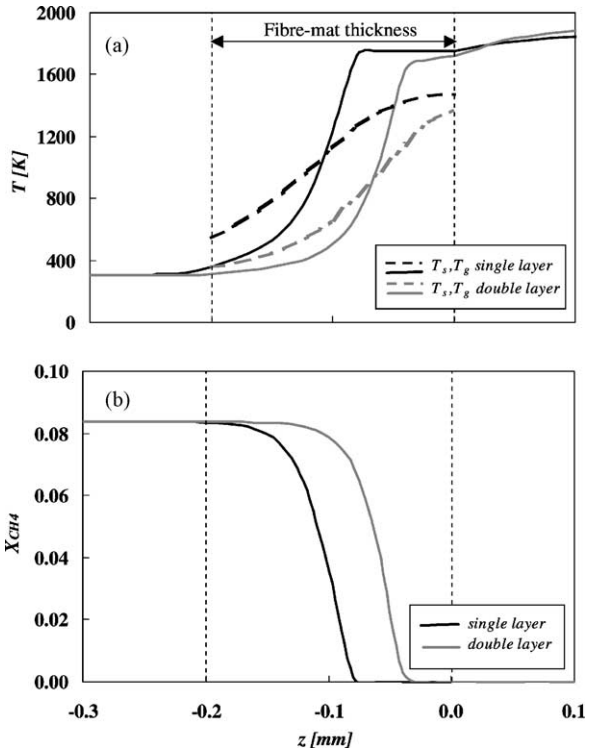


Fig. 11. Calculated thermal profiles (a) and methane concentration profiles (b) for the single-layer structure and for the bi-layered structure ($Q = 500\,\text{kW/m}^2$, $E_a = 15\%$). No catalyst present on both configurations.

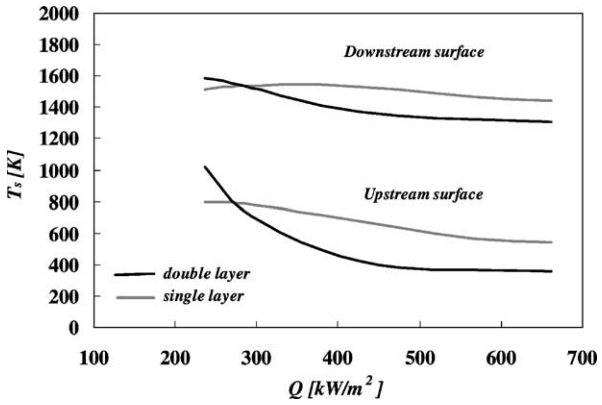


Fig. 12. Surfaces temperature versus $Q$, for the single-layer structure and for the composite structure ($E_a = 15\%$, non-catalytic burner).

thermal conductivity localize the heat thus released. To avoid the detrimental temperature decrease at the upstream surface temperature, a deeper porous medium should be used.

The principal drawback of this configuration resides in the overall pressure drop across the composite porous medium, that could be critical in some particular applications. For instance, the natural gas distribution network in civil areas is characterized by just a small overpressure (about 20–30 mbar). High burner back pressures might thus result in problems in the natural gas feed system.

## 5. Conclusions

A discussion on stability and flashback resistance in metal fiber burners is presented, for both catalytic and non-catalytic systems. The burner model has been first validated against a set of experimental data, at different excess of air and specific power inputs. The principles governing heat transfer in these systems have been discussed, and some major differences between catalytic and non-catalytic systems have been drawn.

A stability analysis was then presented, so as to single out the regions of flashback occurrence and of stable operation. The analysis was based on the presented burner model coupled with an energy balance for the feedstock pre-heating. The comparison between the stability of a catalytic and non-catalytic burners outlined the major issue that affects these systems, especially the catalytic ones, that is flashback. The catalytic activation of the burner makes this problem even more critical.

Since the presence of the catalyst improves the system performance at the expense of a reduction in stability, it is outstandingly important to optimize the burner geometry and the physical properties of the porous medium in order to achieve safe operation with the catalytic burner. In this perspective a sensitivity analysis was carried out on several design parameters: porosity, emissivity, thermal conductivity, fiber diameter. Some conclusions have been drawn:

- A low fiber diameter does not improve much stability but enhances heat transfer efficiency.
- A high emissivity increases the radiation flux; it should be minimized at the upstream surface and maximized downstream.
- A low thermal conductivity increases flashback resistance, but tends to push the flame front outside the porous medium. A trade-off has to be found.
- High porosity increases the system temperature, thus improving performance and reducing stability. A trade-off should be found.

The potential of a composite porous medium has been also discussed, made by a double-layer structure with an upstream radiation shield and a downstream porous mat maximizing radiation. It provides improved performance and flashback resistance. However, the rise in pressure drop it implies, could become an issue and could limit the applicability of this device especially in the domestic appliances.

## Acknowledgements

The financial support of the European Community is gratefully acknowledged (Energy Project HIMOCAT: “High-modulation, high-efficiency and low-emission boilers for household application based on premixed catalytic burners”).

## References

[1] V.C. Kessler, R. Schaaf, O. Menche, On the generation of radicals in premixed porous burners for natural gas, Gas Waerme Int. 36 (1987) 305.
[2] J.A. Gotterba, R.J. Schreiber, R.J. Blair, High efficiency commercial size warm air furnaces using the Alzeta pyrocore burner, in: Proceedings of the Annual Energy Seminar, Erie, PA, 1985, p. 27.
[3] M.D. Rumminger, Numerical and experimental investigation of heat transfer and pollutant formation in porous direct-fired radiant burners, Ph.D. Dissertation, University of California at Berkeley, 1996.
[4] K.J.A. Hargreaves, H.R.N. Jones, D.B. Smith, Developments in burner technology and combustion science, in: Proceedings of the Institution of Gas Engineers Autumn Meeting, Paper No. 1309, London, 1986, p. 31.
[5] G. Saracco, I. Cerri, V. Specchia, R. Accornero, Catalytic premixed fibre burners, Chem. Eng. Sci. 54 (1999) 3599.
[6] R. Sharif, S.V. Pisupati, A.W. Scaroni, Combustion science and technology, in: Kirk-Othmer Encyclopedia of Chemical Technology, 1993.
[7] M. Bizzi, Modelling and operation of short contact time reactors for natural gas conversion, Ph.D. Dissertation, Politecnico di Torino, 2003.
[8] I. Cerri, G. Saracco, V. Specchia, D. Trimis, Improved performance knitted fibre mats as supports for premixed natural gas catalytic combustion, Chem. Eng. J. 82 (2001) 72.
[9] M. Golombok, A. Prothero, L.C. Shirvill, L.M. Small, Gas temperature above a porous radiant burner: comparison of measurements and model predictions, Combust. Sci. Technol. 77 (1991) 233.

[10] A. Kazakov, M. Frenklach, Reduced reaction sets based on GRI-Mech, University of California at Berkeley. http://www.me.berkeley.edu/drm.
[11] R.J. Kee, F.M. Rupley, J.A. Miller, M.E. Coltrin, J.F. Grcar, E. Meeks, H.K. Moffat, A.E. Lutz, G. Dixon-Lewis, M.D. Smooke, J. Warnatz, G.H. Evans, R.S. Larson, R.E. Mitchell, L.R. Petzold, W.C. Reynolds, M. Caracotsios, W.E. Stewart, P. Glarborg, CHEMKIN Collection, Release 3.5, Reaction Design, Inc., San Diego, CA, 1999.
[12] R.J. Kee, G. Dixon-Lewis, J. Warnatz, M.E. Coltrin, J.A. Miller, A Fortran Computer Package for the Evaluation of Gas-phase, Multicomponent Transport Properties, Sandia National Laboratory, SAND86-8246, 1986.
[13] C.T. Bowman, R.K. Hanson, W.C. Gardiner, V. Lissianski, M. Frenklach, M. Goldenberg, G.P. Smith, GRI-Mech 2.11—an optimized detailed chemical reaction mechanism for methane combustion and NO formation and reburning, Gas Research Institute Report, GRI-97/0020, 1997.
[14] O. Deustchmann, R. Schwiedernoch, L.I. Maier, D. Chatterjee, Natural gas conversion in monolithic catalysts: interaction of chemical reactions and transport phenomena, Stud. Surf. Sci. Catal. 136 (2001) 251.
[15] D.A. Hickman, L.D. Schmidt, Steps in $CH_4$ oxidation on Pt and Rh surfaces: high temperature reactor simulations, AIChE J. 39 (1993) 1164.
[16] D. Trimis, University of Erlangen, Private communication, 2001.
[17] O. Deutschmann, L.D. Schmidt, Modelling the partial oxidation of methane in a short contact time reactor, AIChE J. 44 (1998) 2465.
[18] T.H. Chilton, A.P. Colburn, Mass transfer (absorption) coefficients: prediction from data on heat transfer and fluid friction, Ind. Eng. Chem. 26 (1934) 1183.
[19] M.D. Rumminger, R.D. Hamlin, R.W. Dibble, Numerical analysis of a catalytic radiant burner: effect of catalyst on radiant efficiency and operability, Catal. Today 47 (1–4) (1999) 253.